Post-shock downstream evolution of turbulent boundary layer based on quadrant analysis

M. F. Shahab[a], G. Lehnasch[a], T. B. Gatski[a,b], P. Comte[a]

a. *Institute Pprime*
Department of Fluid Flow, Heat Transfer and Combustion
Université de Poitiers, ENSMA, CNRS
b. *Center for Coastal Physical Oceanography and Ocean, Earth and Atmospheric Sciences*
Old Dominion University, Norfolk, Virginia 23529 USA

Résumé :

Une décomposition par l'analyse en quadrants des fluctuations de vitesse a été effectuée afin de quantifier la présence des différent événements turbulents (par exemple, éjections et balayages) dans une couche limite supersonique turbulente perturbée par un choc oblique. Dans la présente analyse, le comportement post-choc de la couche limit supersonique perturbé est comparée avec les résultats obtenus en amont de l'interaction. L'effet de la condition à la paroi (isotherme froid vs adiabatique) sur les éjections et balayages est également étudié.

Abstract :

A quadrant analysis decomposition of velocity fluctuations has been performed in order to quantify the occurrence of different turbulent events (e.g. ejections and sweeps) in a supersonic turbulent boundary layer perturbed by an oblique shock. In the present analysis, the post-shock behavior of the perturbed turbulent boundary is compared with the results obtained upstream of the interaction. The effect of wall boundary condition (isothermal cold-wall versus adiabatic) on the burst and sweep events is also investigated.

Mots clefs : supersonic flow ; shock-interactions ; quadrant analysis

1 Introduction

A quadrant analysis is used to investigate the effect on the turbulent structure that occurs within the compressible turbulent boundary layers perturbed by a strong flow discontinuity (shock-wave). Direct numerical simulations of spatially evolving turbulent boundary layers at Mach =2.25 with an impinging shock-wave (flow deflection angle of 8°) have been performed. In addition to the adiabatic wall, zero heat flux condition, a simulation based on the isothermal cold-wall temperature condition has also been included in the present analysis. The reference flow simulations case has no-shock, and has been thoroughly analyzed and reported in the earlier publications of the authors ([5, 6]).

Statistics are gathered using 2500 flow-field sets at 6 different streamwise stations (1 plane upstream of the shock-system and the rest of them are in the relaxation region downstream of the incident shock impingement point) extending over a total time period of $65\delta_c^o/U_\infty$(where δ_c^o designates the boundary layer thickness at the reference station $P01$). A numerical schlieren snapshot of the flow-field is presented in Fig. 1 in order to illustrate the enhancement of turbulent structures and the change of flow dynamics that occur as a consequence of interaction with the shock-system, and also to indicate the positions of the diagnostic planes used in the present analysis. The physical and numerical parameters for the present study are detailed in Table 1, while the positions of the diagnostic planes are summarized in Table 2.

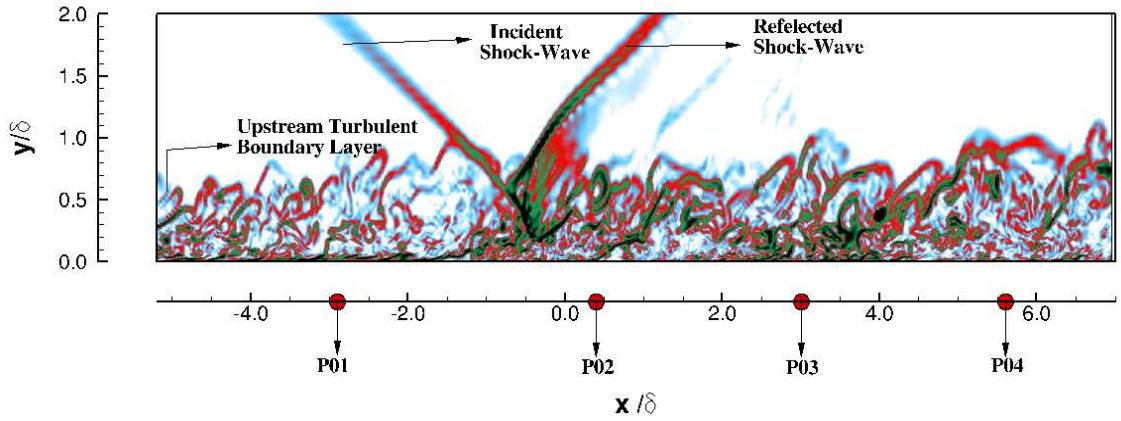

FIGURE 1 – Instantaneous numerical schlieren plot for the present direct numerical simulation along with the relative location of the diagnostic planes. Note : the out of range stations $P05$ and $P06$ are situated at $x/\delta_c^o = 8.2$ and 16.8 respectively.

TABLE 1 – Parameter specification : (a) Physical parameters ; (b) Numerical parameters.

(a) Adiabatic Case

Wall Condition	M_∞	$Re_\infty/m.$	Re_θ	H
Adiabatic	2.25	25×10^6	3390	3.40
Isothermal	2.25	25×10^6	3775	2.65
Wall Condition	T_∞	B_q	M_τ	T_w
Adiabatic	170K	0.0	0.077	323K
Isothermal	170K	-0.017	0.079	230K

(b) Numerical parameters

Wall Condition	N_x	N_y	N_z
Adiabatic	2650	111	255
Isothermal	2650	111	255
Wall Condition	Δx^+	Δy_w^+	Δz^+
Adiabatic	13.90	0.76	6.50
Isothermal	22.05	1.19	10.30

TABLE 2 – Positions of diagnostic planes (x_i is the impingement position of incident shock-wave, and δ_c^o is the boundary layer thickness at reference station $P01$).

Plane	$xpos = (x - x_i)/\delta_c^o$	
	Adiabtic	Isothermal
$P01$	-2.9	-2.9
$P02$	0.4	0.4
$P03$	3.0	3.0
$P04$	5.6	5.6
$P05$	8.2	8.2
$P06$	16.7	16.7

2 Quadrant Analysis Method

Quadrant analysis is one technique that is commonly used to detect and to quantify the occurrence of different turbulent events (e.q ; ejections and sweeps) in a turbulent boundary layer. As proposed by Lu & Willmarth [7], the technique involves the splitting of the u'-v' velocity plane into four quadrants according to the signs of the velocity fluctuations (u' and v'). The events associated with the instantaneous Reynolds shear stresses ($(u'v')_i$) can then be detected by identifying the stresses with their corresponding quadrant based on the signs of fluctuations. On the basis of this conditional sampling,

the averages in each quadrant are estimated by using the following expression

$$(\overline{u'v'})_i = \frac{1}{N}\sum_{j=1}^{N} S_i \times (u'v')_j, \tag{1}$$

where $S_i = 1$ is the point $(u'v')_j$ in the ith quadrant, $S_i = 0$ otherwise, and N is the number of data samples at each point of consideration. The turbulent events relative to each u'-v' quadrant are defined as follows : the first quadrant, where $u' > 0$ and $v' > 0$ contains the events associated with the outward motion of high-speed fluid ; the second quadrant, where $u' < 0$ and $v' > 0$ contains the events that are associated with the ejections (or bursts) of low-speed fluid away from the wall ; the third quadrant, where $u' < 0$ and $v' < 0$ represents the events corresponding to the inward motion of low-speed fluid ; and the fourth quadrant, where $u' > 0$ and $v' < 0$, represents the events that characterize the sweeping of high-speed fluid towards the wall. The sketch presented in Fig. 2 summarizes the above discussion about the turbulent events.

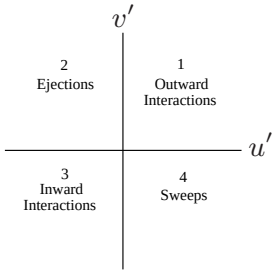

FIGURE 2 – The four quadrants of $u' - v'$ plane

3 Results & Discussion

The joint probability density functions($j.p.d.f$) associated with the streamwise and wall-normal components of the velocity fluctuations are shown in Fig. 3. The j.p.d.f's are plotted at a fixed streamwise station ($stationP01$) upstream of the interaction, showing their wall-normal variation in the boundary layer. All the displayed j.p.d.f's indicate that the distribution of $u' - v'$ velocity fluctuations are represented by the characteristic ellipses that are centered around the origin of the $u' - v'$ plane, and their major axes situated in the second and the fourth quadrants (except the one which is very near to the wall – Fig. 3a-I). The representation of the j.p.d.f's in the logarithmic region (Fig. 3a-II,III) closely resembles the scatter data representation of the velocity fluctuations found by Deleuze [2] for the case of an adiabatic supersonic turbulent boundary layer. In addition, a qualitative comparison with the incompressible channel flow results of Kim et al. [3] also shows the alignment of the major axis of the ellipse with the u'-axis in the near-wall region of the boundary layer and further demonstrates the dominance of the streamwise velocity fluctuations over the wall-normal fluctuations

Figure 4a shows the downstream evolution of the contributions of the conditionally averaged Reynolds shear stresses ($\overline{u'v'}_i$) across the boundary layer for the adiabatic case, in comparison with their values upstream of the interaction (Profile P01). The results presented here are normalized with the respective total turbulent shear stress ($\overline{u'v'}$) in order to determine the relative contribution of each quadrant. Upstream of the interaction (Profile $P01$), the trends obtained here are in qualitative agreement with the observations made in incompressible and compressible wall-bounded flows ([3], [1], [4]). The dominant contributions to the Reynold shear stress ($\overline{u'v'}$) are from the second and fourth quadrants, that is, the ejections and sweeps. Furthermore, it is noted that in a large part of the boundary layer ($0.1 < y/\delta_c^l < 0.5$), upstream of the interaction, the conditional averages do not show a large variation. The second notable attribute is the fact that away from the wall, ejection events show their dominance over all the other contributors ; however, very near the wall ($y/\delta_c^l < 0.02$), the sweeps are found to be the largest contributor. On average, the ejections add a 73% share to the Reynold shear stress ($\overline{u'v'}$), with sweeps accounting for 57%. The remaining 30% negative contributions are from the first and third quadrants

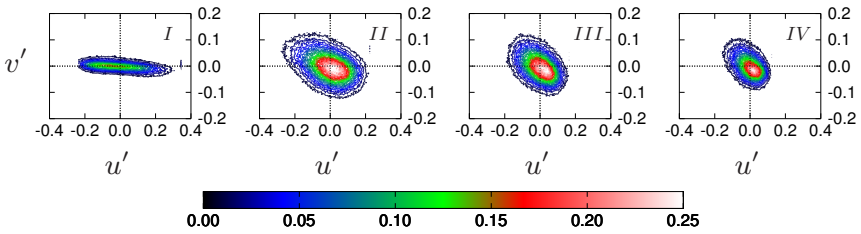

(a) Adiabatic Case

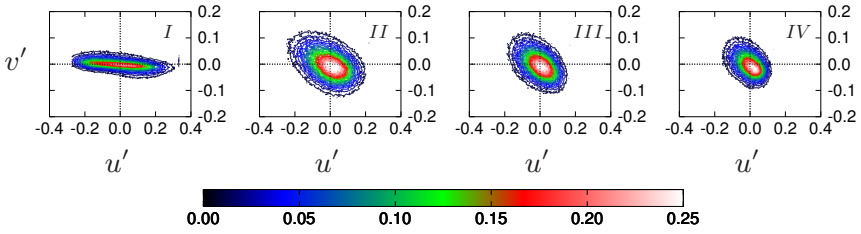

(b) Isothermal Case

FIGURE 3 – Joint probability distribution : (a) Adiabatic ; (I) $y/\delta_c^o = 0.012$, $y^+ = 8.5$; (II) $y/\delta_c^o = 0.071$, $y^+ = 51.5$; (III) $y/\delta_c^o = 0.246$, $y^+ = 178.2$; (IV) $y/\delta_c^o = 0.44$, $y^+ = 315.3$ (b) Isothermal ; (I) $y/\delta_c^o = 0.012$, $y^+ = 13.4$; (II) $y/\delta_c^o = 0.071$, $y^+ = 81.5$; (III)$y/\delta_c^o = 0.246$, $y^+ = 281.8$; (IV)$y/\delta_c^o = 0.44$, $y^+ = 498.0$

(note this average is based on the region $0.1 < y/\delta_c^l < 0.5$ at the station upstream of the interaction, P01, and δ_c^l designates the boundary layer thickness at each local station). The percentage decomposition of the total turbulent shear stress ($\overline{u'v'}$), in terms of the conditional Reynolds stress components described above, shows a reasonable agreement with the results found in the literature. For example, Lu and Willmarth [7] indicated the following composition : -15% first quadrant, 77% second quadrant, 17% third quadrant, and 55% fourth quadrant, while Deleuze et al. [1] reported a composition : -5% first quadrant, 60% second quadrant, -5% third quadrant, and 50% fourth quadrant.

Downstream of the interaction($P02 - P06$), a notable change in the ejection and sweep contributions is observed, and the cross-over point between second (ejections) and fourth (sweeps) quadrant distributions move away from the wall, this observation has also been reported by Deleuze ([2]) in a turbulent boundary layer shock impingement study. In addition, the sign reversal behavior found in the skewness factors (Fig. 5, Fig. 6) evolution, downstream of the interaction, is also consistent with the present observation. Deleuze [2] also reported the same sign reversal behavior after the interaction with an impinging shock-wave which shows that the positive values of u' are more frequent than the negative values when compared to the trends observed before the interaction and vice-versa for the v'. This observation leads to the conclusion that in the interaction with the shock, the contribution of sweep events in the boundary layer is enhanced and the extent through which they act across the boundary layer is enhanced. The distortion produced by the shock relaxes with increased distance in the recovery zone and the results obtained at the station $P06$ shows a set of unstrained conditional Reynolds stress distributions similar to that of the undisturbed boundary layer.

For the isothermal case (Fig. 4b), the average percentage composition of each quadrant is similar to that of the adiabatic case. Moreover, downstream of the interaction, the region where sweeps remain dominant over the ejections is comparatively less in the isothermal case than in the adiabatic case. Also, the relaxation distance is relatively short in the isothermal cold-wall case.

In order to further clarify the changes that occur in the contributions of the ejection and sweep events downstream of the interaction, the ratios of second (ejections) and fourth (sweeps) quadrant events are plotted in Fig. 7 along with the distribution in the undisturbed boundary layer. The ratio of $(\overline{u'v'})_2/(\overline{u'v'})_4$ in the undisturbed boundary layer (Profile $P01$) shows a qualitative and comparable quantitative agreement with the results obtained by Deleuze [2] and Lu and Willmarth [7]. It is clear that upstream of the interaction, over most of the boundary layer, the ejections make the largest contri-

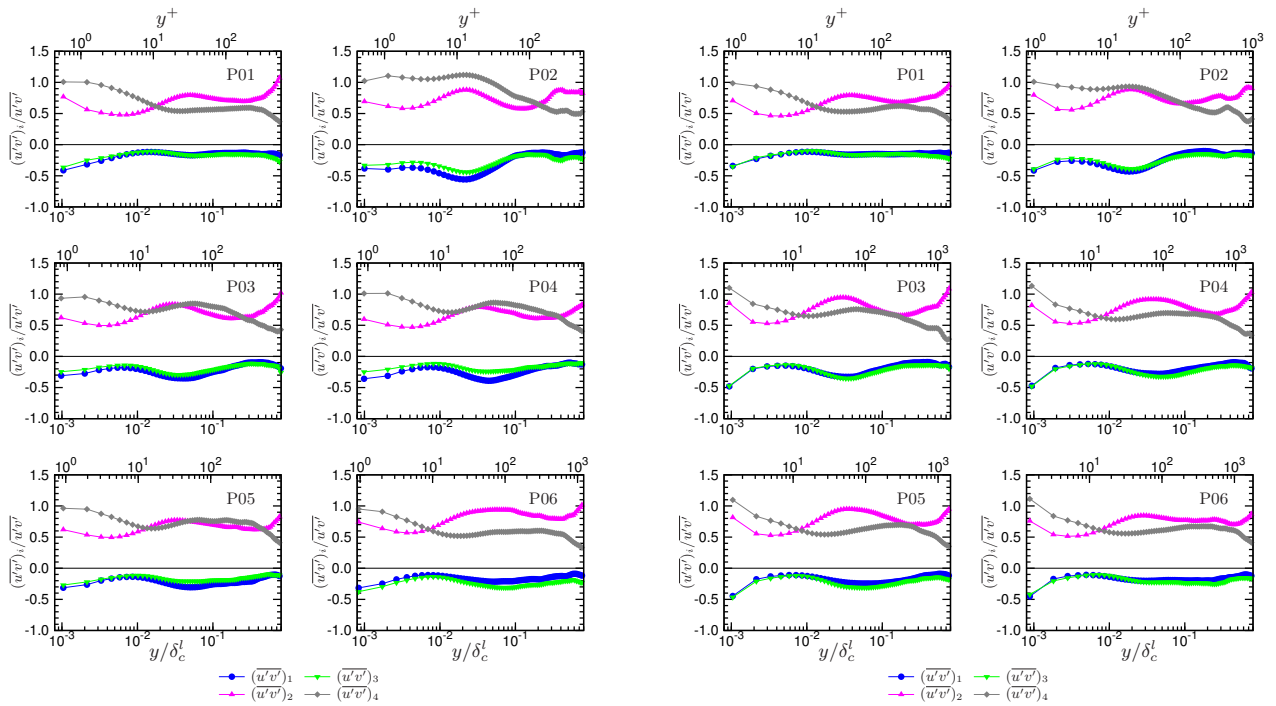

(a) Adiabatic Case (b) Isothermal Case

FIGURE 4 – Quadrant analysis across the boundary layer : (a) Adiabatic ; (b) Isothermal (Note : Bottom x-axis represents the scale in y/δ_c^l units while the corresponding values in y^+ units are indicated on the top x-axis)

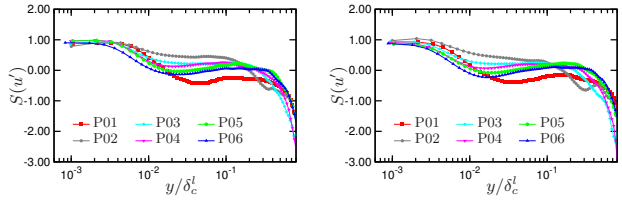

(a) Adiabatic Case (b) Isothermal Case

FIGURE 5 – Skewness factor variation across the boundary layer, u-component : (a) Adiabatic ; (b) Isothermal

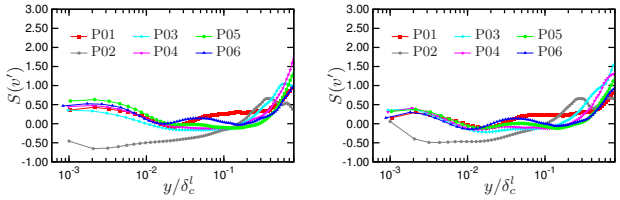

(a) Adiabatic Case (b) Isothermal Case

FIGURE 6 – Skewness factor variation across the boundary layer, v-component : (a) Adiabatic ; (b) Isothermal

bution ; however, very near the wall, the sweep events show their dominance. This drop-off in the values of $(\overline{u'v'})_2/(\overline{u'v'})_4$ in the very near wall region ($\delta_c^l < 0.02$) is not observed by [2] and [7] due to the unavailability of data in this region. However, the behavior is characteristic of turbulent boundary layers, as Kim et al. [3] and Wallace et al. [4] have also indicated that sweeps are more predominant in the near wall region than the ejections. In the region, $\delta_c^l > 0.6$, the ratio $(\overline{u'v'})_2/(\overline{u'v'})_4$ increases in a rapid fashion due to the prevailing rise of the ejection events and the pronounced decrease in the sweep contributions.

The affect of the interaction on the ratio of $(\overline{u'v'})_2/(\overline{u'v'})_4$ is clear from the distribution of the profiles $P02 - P06$. The shifting of the cross-over point between the second and fourth quadrant distributions away from the wall (Fig. 4) causes the ratio to drop slightly less than one, and is consistent with the conclusion of Deleuze [2] for the case of turbulent boundary layer interaction with an impinging shock. For the isothermal case, it appears that the effect of interaction is limited in the recovery zone and the relaxation process is more rapid than in the adiabatic case.

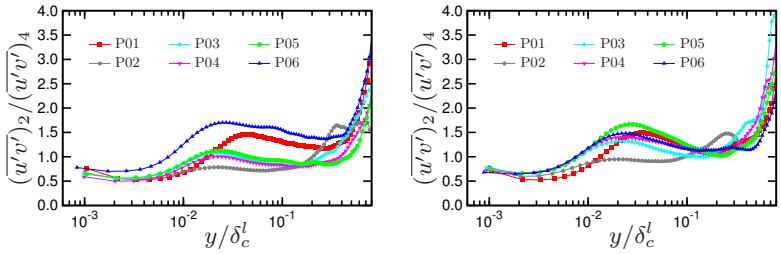

(a) Adiabatic Case (b) Isothermal Case

FIGURE 7 – Ratio of $(\overline{u'v'})_2$ (ejections) over $(\overline{u'v'})_4$ (sweeps) across the boundary layer : (a) Adiabatic ; (b) Isothermal

4 Conclusions

The distributions of the conditionally averaged shear stresses shows a global similarity with the distributions observed in the literature for the case of compressible and incompressible turbulent boundary layers. In most of the boundary layer upstream of the interaction, ejection events are more prevalent over the other contributions, except very near to the wall where sweep events shows their domination. The effect of the interaction enhances the extent in the boundary layer over which the sweep contributions dominate over the ejections. The effect of isothermal wall condition is to shorten the relaxation distance.

Acknowledgements : M.F.Shahab acknowledges the support of the Higher Education Commission Pakistan. This work was performed using HPC resources from GENCI- [CCRT/CINES/IDRIS] (Grant 2011- [x2011090912]) under the support of the Agence Nationale de la Recherche (SPICEX project (ANR-07-CIS7-009)).

Références

[1] J. Deleuze and N. Audiffren and M. Elena 1994 Quadrant analysis in a heated-wall supersonic boundary layer. *Phys. Fluids* **6(12)** 4031-4041

[2] J. Deleuze 1995 Structure d'une couche lite turbulente soumise à une onde de choc incidente. *Ph.D Dissertation Université de la Mediterranee Aix - Marseille*

[3] J. Kim and P. Moin and R. Moser 1987 Turbulence statistics in fully developed channel flow at low Reynolds number. *J. Fluid Mech.* **177** 133-166

[4] J. M. Wallace and H. Eckelmann and R. S. Brodkey 1972 The wall region in turbulent shear flow. *J. Fluid Mech.* **54** 39-48

[5] M. F. Shahab and G. Lehnasch and T. B. Gatski and P. Comte 2011 Statistical characteristics of an isothermal supersonic developing boundary layer flow from DNS Data *Flow Turbulence Combust.* **DOI 10.1007/s10494-011-9329-0**

[6] M. F. Shahab and G. Lehnasch and T. B. Gatski and P. Comte 2010 Influence of wall cooling on the statistics of a supersonic turbulent boundary layer flow. *In* 8^th *International ERCOFTAC Symposium on Engineering Turbulence Modelling and Measurements,France*

[7] S. S. Lu and W. W. Willmarth 1973 Measurements of the structure of the Reynolds stress in a turbulent boundary layer. *J. Fluid Mech.* **60** 481-511